Int. J. Nanosci. Nanotechnol., Vol. 7, No. 2, Jun. 2011, pp. 65-71

Electronic Properties of a Concentric Triple Quantum Nanoring

H. K. Salehani[1], M. Esmaeilzadeh[2*], Kh. Shakouri[2], M. R. Abolhassani[1], E. Faizabadi[2], and M. H. Majlesara[3]

1- Plasma Physics Research Center, Science and Research Branch, Islamic Azad University, Tehran, I.R. Iran
2- Department of Physics, Iran University of Science and Technology, Tehran, I.R. Iran
3- Department of Physics, Faculty of Science, Tarbiat Moallem University, Tehran, I.R. Iran

(*) Corresponding author: mahdi@iust.ac.ir
(Received: 05 Jan. 2011 and Accepted: 18 Apr. 2011)

Abstract:
In this paper, we study the electronic properties of a concentric triple quantum ring using exact diagonalization technique. The energy spectra and magnetization for a single electron and two electrons, in the presence of an applied magnetic field, are calculated and discussed. It is shown that, for two-interacting electrons, the period of Aharonov-Bohm oscillations decreases to the half of that for non-interacting electrons which shows the fractional Aharonov-Bohm oscillations for interacting electrons. It is found that the spin-singlet state for two electrons is more stable than the spin-triplet states. Also, magnetization effect decreases due to the electron-electron interaction.
Keywords: *Quantum rings, Electronic properties, Energy spectra, Magnetic flux.*

1. INTRODUCTION

Over the last two decades, the study of quantum dots as tunable artificial atoms and quantum ring structures which exhibit the Aharonov-Bohm effect, have attracted great interest [1-6]. Quantum rings (QRs), which stand as an alternative to quantum dots (QDs) for eventual use in nanotechnology devices, are small conductor or semiconductor rings with few electrons. The size of QRs is of order of the phase-coherence length of electrons. A noticeable difference between the QDs and QRs arises from their topology that causes QRs display interesting phenomena such as persistent current which are not found in QDs. Double quantum rings (DQRs) structures can be considered as "artificial diatomic molecules" [7-9]. One type of DQRs that has attracted the interest of researchers during the last few years is concentric DQRs. The concentric DQRs have been fabricated by using droplet epitaxial growth [7, 10] as well as atomic force microscope tip oxidation techniques [11, 12].

In a number of theoretical works, DQRs with different configurations have been investigated [8, 13-21]. The effect of coupling between the rings on the energy spectrum of a single electron has been studied by Fuster *et al.* [13]. Szafran and Peeters have studied energy spectra of a concentric DQR with 1-3 electrons [14]. The previous works on concentric DQRs have been extended by Climente *et al*. to investigate the ground state structure of self-assembled DQRs [15]. Planelles *et al.* have studied the electronic states of DQRs, for lateral configuration, within the frame of the effective mass

envelope function theory [19]. Chwiej and Szafran have investigated artificial molecular states formed in DQRs with the same configuration for a single electron as well as two and three electrons [8]. The electronic localization for few electrons in concentric DQRs in the presence of perpendicular magnetic field has been studied by Escartıin *et al.* [21].
Recently, fabrication of GaAs/AlGaAs concentric triple quantum rings (TQRs) has been reported by Somaschini *et al*. using an innovative growth method based on droplet epitaxy [22]. This motivated us to study electronic properties of TQRs. In a recent paper, we have studied the effects of donor impurity on energy spectra and energy gaps in a TQR [23]. In that study, the electron-electron interaction has been ignored. The present work is an extension of the above study to investigate the effects of electron-electron interaction on energy spectra, Aharonov-Bohm oscillations and magnetization in a TQR. The effects of inter-ring coupling for single electron in a TQR are also investigated in the present work. It is shown that Aharonov-Bohm oscillations with fractional period appear due to the electron-electron interaction. Also, electron-electron interaction decreases the magnetization and increases the energy levels. The organization of this paper is as fallows: A theoretical model is presented in Sec. 2. The results of a numerical study are presented and discussed in Sec. 3. Finally, a summary and conclusions are given in Sec. 4.

2. THEORETICAL MODEL

In this section, a theoretical model for a coupled concentric TQR is presented. We assume that the vertical confinement is such narrow that the TQR can be considered as a two-dimensional system. The confinement potential of TQR is assumed to be parabolic as shown in figure 1. The single electron Hamiltonian in the presence of a magnetic field applied perpendicularly to the TQRs plane (i.e., $\mathbf{B} = B\hat{\mathbf{e}}_z$) may be written as

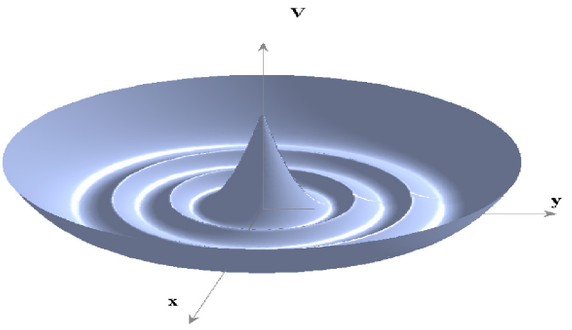

Figure 1: *Schematic view of a parabolic confinement potential for a coupled concentric TQR*

in the polar coordinates, where m^* is the effective mass of the electron, ρ is the electron radial distance from the center of rings, L is the quantum number of the angular momentum, $\omega_c \equiv eB/m^*$ is the cyclotron frequency and

$$V(\rho) = \frac{1}{2} m^* \min[\omega_1^2(\rho - R_1)^2, \omega_2^2(\rho - R_2)^2, \omega_3^2(\rho - R_3)^2] \quad (2)$$

is the parabolic confinement potential. In Eq. (2), ω_1, ω_2 and ω_3 are the confinement potential strengths for internal, middle and external rings and R_1, R_2 and R_3 are their corresponding radii, respectively. The second term in Eq. (1) is the centrifugal potential and the third and fourth ones are the diamagnetic and orbital Zeeman potentials, respectively. Note that the effect of the spin Zeeman potential is neglected in the present study. Using Eq. (1), the few electrons Hamiltonian can be written as

$$H = \sum_{i=1}^{N} H_0(\rho_i) + \sum_{i=1}^{N} \sum_{j>i}^{N} \frac{e^2}{4\pi\varepsilon\varepsilon_o |\vec{\rho}_i - \vec{\rho}_j|} \quad (3)$$

where the first term in Eq. (3) is the Hamiltonian of N non-interacting electrons and the second one is the Coulomb interaction between electrons. Here,

$$H_0 = -\frac{\hbar^2}{2m^*}\left(\frac{d^2}{d\rho^2} + \frac{1}{\rho}\frac{d}{d\rho}\right) + \frac{\hbar^2 L^2}{2m^*\rho^2} + \frac{m^*\omega_c^2\rho^2}{8} - \frac{1}{2}\hbar\omega_c L + V(\rho) \quad (1)$$

ε is the dielectric constant, ε_o is the permittivity of vacuum and ρ_i is the position vector of i[th] electron.

3. NUMERICAL STUDY AND DISCUSSION

The wave functions and energy spectra of a single electron and few electrons are calculated numerically by using finite difference and exact diagonalization method [14]. For numerical calculations, the radius of rings are taken to be R_1=40 nm, R_2=70 nm and R_3=105 nm and the width of rings are taken to be d_1=20 nm, d_2=25 nm and d_3=30 nm corresponding to the concentric TQR fabricated recently [22]. We choose the GaAs values for dielectric constant and electron effective mass (i.e., $\varepsilon = 12.4$ and $m^* = 0.067\, m_e$ where m_e is the free electron mass). The confinement strength of internal, middle and external rings can be calculated by using $\omega_1 = 2\hbar / m^* l_1^2$, $\omega_2 = 2\hbar / m^* l_2^2$, $\omega_3 = 2\hbar / m^* l_3^2$ where $l_1 = d_1/2$, $l_2 = d_2/2$ and $l_3 = d_3/2$ are the half-width of the internal, middle and external rings, respectively [13,14]. This yields $\hbar\omega_1 = 22.8 meV$, $\hbar\omega_2 = 14.6 meV$ and $\hbar\omega_3 = 10.13 meV$.

3.1. Single electron

Now, we calculate the energy spectrum and probability density of a single electron using Hamiltonian in Eq. (1). The electron probability density (i.e., $\rho|\phi|^2$) of the lowest state in the absence of the centrifugal potential (L=0) is shown in figure 2 for different magnetic fields B=0, 1.3 and 2.3T. It is clear that for B=0, 1.3 and 2.3T the electron wave function is approximately localized in the external, middle and internal rings, respectively. The effect of the centrifugal potential on the electron probability density is shown in figure 3 for a constant magnetic field B=2.3T and for different angular momenta L=0, 10 and 13. As this figure shows, unlike the previous case, the lowest electron wave function for L=0, 10 and 13 is approximately localized in the internal, middle and external rings, respectively. By comparing figures 2 and 3, one can find that the centrifugal and diamagnetic potentials act opposite to each other. In the other words, the

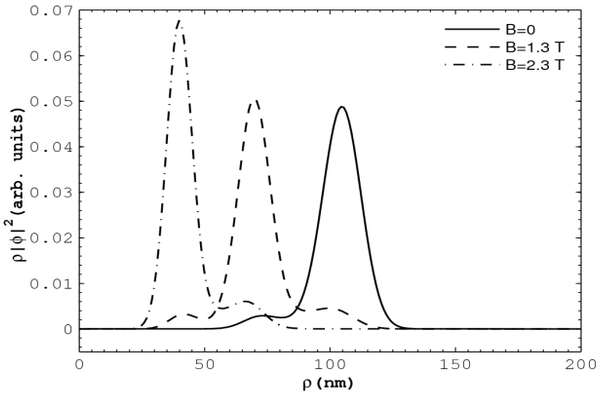

Figure 2: *The single electron probability density of the lowest state with radii R_1=40 nm, R_2=70 nm and R_3=105 nm as a function of radial distance for L=0 and different magnetic fields B=0, B=1.3T and B=2.3 T.*

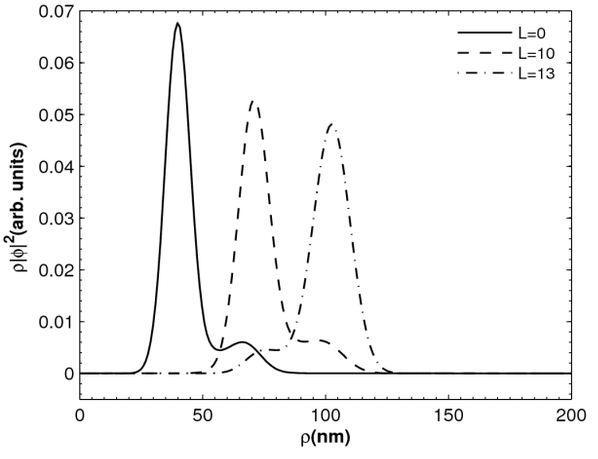

Figure 3: *The single electron probability density of the lowest state in a TQR as a function of radial distance for B=2.3T and different angular momenta L=0, L=10 and L=13.*

diamagnetic potential causes the electron to localize in the inner rings, while the centrifugal potential causes the electron to localize in the external rings. The single-electron energy spectrum as a function of the external magnetic field is plotted in figure 4 for different angular momenta L=0, 1, 2,…, 6 (a) for a TQR and (b) for three isolated single QRs with the radii and confinement strengths same as the TQR. In figure 4(a), solid, dashed and dash-dotted

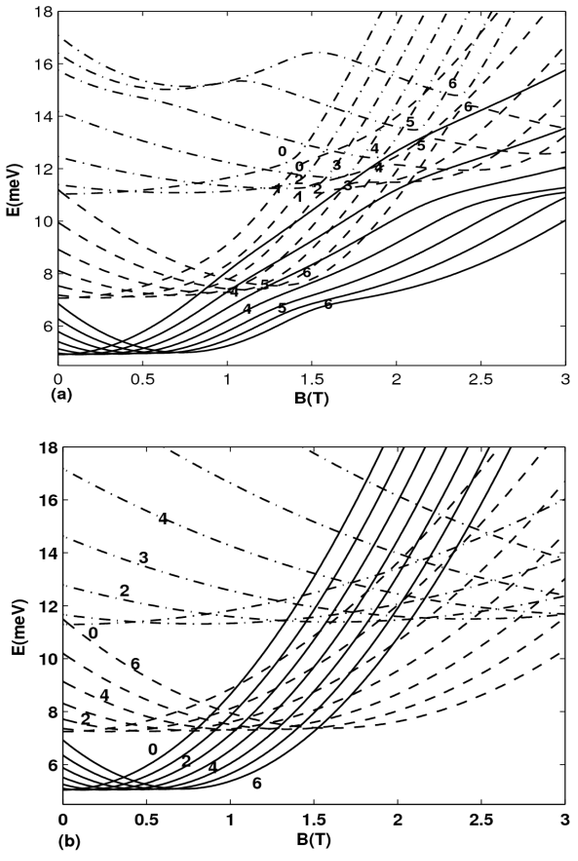

Figure 4: *The single-electron energy spectrum as a function of magnetic field for different quantum numbers of angular momentum (i.e., L=0, 1,… , 6). (a) for a TQR and (b) for three isolated single quantum rings with the radii and confinement strengths same as the TQR.*

curves indicate the first, second and third lowest states of each quantum number *L*, respectively. The energy levels corresponding to different quantum numbers of angular momentum up to 6 are plotted with different colors. As figure 4(a) shows, for each angular momentum *L*, there is an anticrossing between the first and second energy levels as well as between second and third energy levels. The energy distance between the first and second energy levels at anticrossing points is greater than the energy distance between the second and third levels. As we see in figure 4(b), in contrast with TQR, there is no any anticrossing between energy levels with the same angular momenta for three isolated rings. Therefore, the anticrossings are induced due to the inter-ring coupling between the rings in a TQR.

3.2. Few-electron system

The electronic properties of few electrons are investigated in this subsection by solving the few-electron Schrodinger equation numerically [Eq. (3)]. The basis set of few-electron Hamiltonian is constructed using the single-electron eigenstates in the form of the Slater determinant [14]. The elements of the Coulomb potential matrix can be calculated by numerical integration of the Coulomb potential over the basis set. Here, we only study the electronic properties of a TQR with two electrons.

Figure 5 shows the two-electron energy spectrum corresponding to different quantum numbers of total angular momentum as a function of the magnetic field (a) in the absence of Coulomb interaction (non-interacting electrons) and (b) in the presence of Coulomb interaction (interacting electrons). The solid curves indicate the energy levels for the spin-singlet state and the dashed curves indicate the energy levels for spin-triplet states. It is observed that for the two non-interacting electrons, the ground-state takes only even numbers of the total angular momentum (i.e., 0, 2, 4, …), while for the interacting case the ground state takes all integer (odd and even) numbers of total angular momentum. In addition, for the non-interacting electrons, the ground state includes only spin-singlet state whereas, for the interacting electrons the ground state is switched between singlet and triplet states, alternatively. In the absence of the Coulomb interaction, for the odd quantum numbers of the total angular momentum, the energy levels with spin-singlet state (curves with circle marks) and spin-triplet states (curves with triangle marks) coincide with each other while for the even quantum numbers they are separated [solid and dashed curves in Figure 5 (b)]. Thus, in the case of non-interacting electrons, the intersections in the ground state are six-fold degenerate but in the interacting case, the degeneracy decreases and the intersections are two-fold or four-fold degenerate. Note that the spin-triplet states are three-fold degenerate.

To see the effect of the Coulomb interaction on two-electron system clearly and compare it with

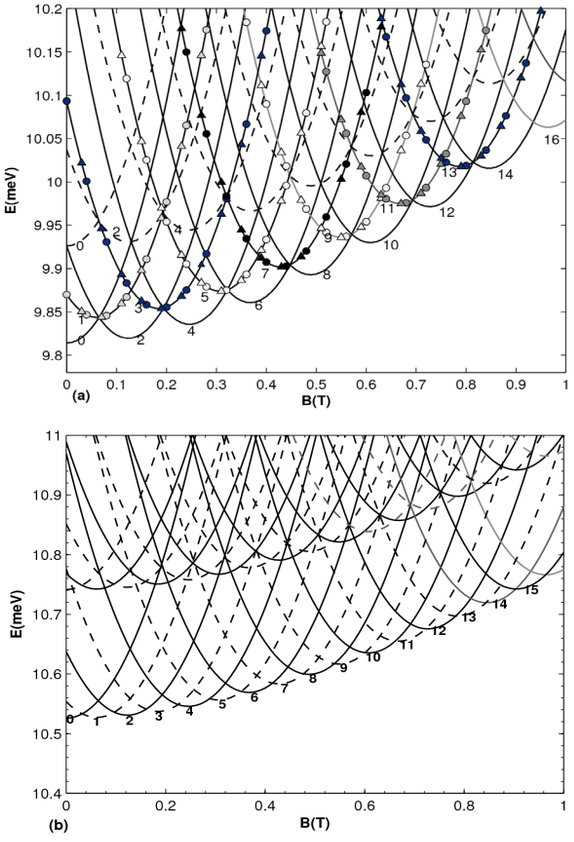

Figure 5: *The two-electron energy spectrum as function of the magnetic field for different quantum numbers of total angular momentum L=0, 1, …, 16. (a) for non-interacting electrons and (b) for interacting electrons. The solid curves indicate the energy levels for the spin–singlet state and the dash-dotted curves are for the spin-triplet states.*

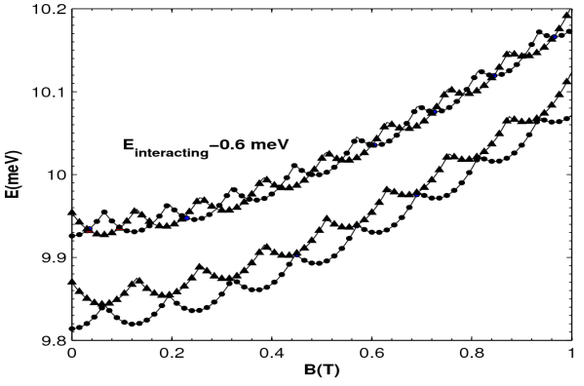

Figure 6: *The two lowest energy levels of two interacting (upper graphs) and two non-interacting electrons (lower graphs) as a function of the magnetic field. The circle marks indicate the spin-singlet state and the triangle marks are for the spin-triplet states.*

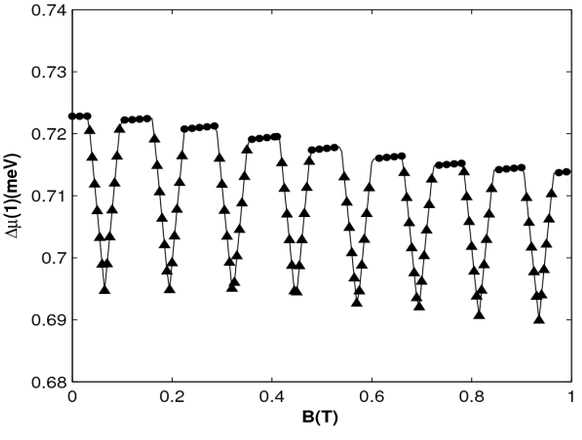

Figure 7: *The chemical potential difference or addition energy as a function of the magnetic field. The circle marks show the addition energy of the spin-singlet state and the triangle marks show the addition energy of spin-triplet states.*

non-interacting system, the energy levels of the two lowest states (ground and first excited states) are shown in figure 6. The circle marks show the spin-singlet state and the triangle marks represent the spin-triplet states. In this figure, the upper graphs indicate the energy levels of the two-interacting electrons and the lower ones indicate the energy levels of two non-interacting electrons. As it is seen, the period of Aharonov-Bohm oscillations for interacting case is the half of that for non-interacting case which shows the fractional Aharonov-Bohm oscillations for interacting system. It is also apparent that the electron-electron interaction significantly increases the energy levels relative to the non-interacting case.

Now, we investigate the addition energy and magnetization in a TQR. In figure 7, the chemical potential difference $\Delta\mu$ is plotted versus the magnetic field. Note that the chemical potential difference can be defined as $\Delta\mu(N) = \mu(N+1) - \mu(N)$ where $\mu(N) = E(N) - E(N-1)$ and $E(N)$ is the N

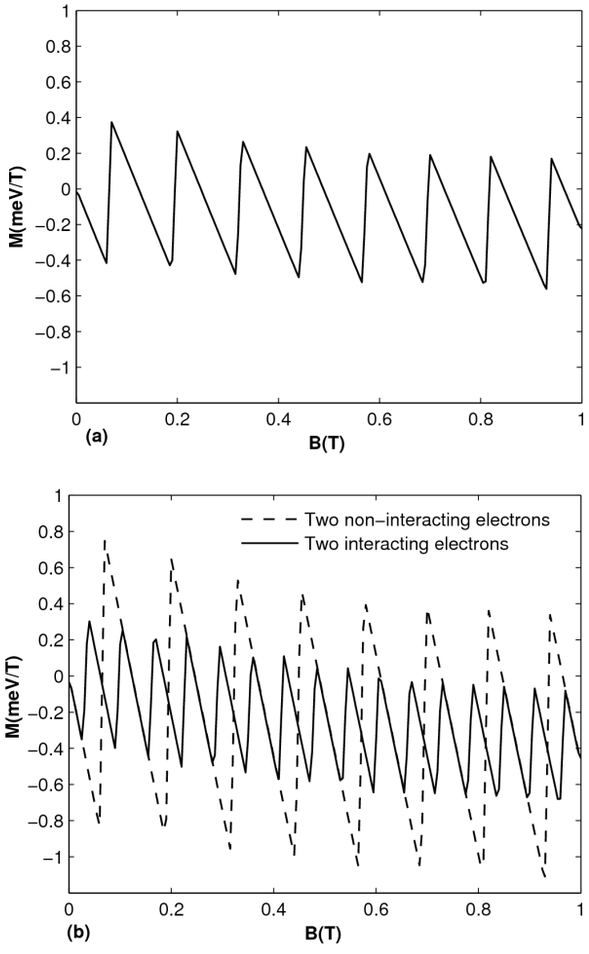

Figure 8: *The magnetization as a function of the magnetic field, (a) for a single electron and (b) for two electrons.*

electrons ground state energy. This difference corresponds to an energy required to add one more electron into the TQRs containing *N* electrons which is referred to "addition energy". It is evident from this definition that an eigenstate with larger addition energy is more energetically stable than that with lower addition energy. In figure 7, the circle marks indicate the addition energy for spin-singlet state and the triangle marks show addition energy for the spin-triplet states. As figure 7 shows, the addition energy for spin-singlet state is higher than that for spin-triplet states. Therefore, it can be concluded that the spin-singlet state for two-electron system are more stable than the spin-triplet states.

Similar to the calculation of the magnetization in a self-assembled single QR [24], it is possible to calculate the magnetization in a concentric TQR. Using Byers-Yang relation, the magnetization of a TQR at zero temperature can be written as [25]

$$M(B) = \sum_{\substack{all\ occoupied \\ states\ i}} -\frac{\partial E_i}{\partial B} \tag{4}$$

Figure 8 shows the magnetization in a TQR, (a) for a single electron and (b) for two electrons. In figure 8(b), the solid and dashed curves show the magnetization for interacting and non-interacting electrons, respectively. As figure 8 shows, for both single and two-electron systems, the magnetization oscillates with increasing magnetic field. Also, it can be seen that the electron-electron interaction decreases the amplitude and oscillation period of magnetization for the two-electron system. In the other words, the magnetization decreases due to the electron-electron interaction.

4. SUMMARY AND CONCLUSION

A theoretical study has been presented for electronic properties of a TQR in the presence of magnetic field perpendicularly applied to the TQR plane. The eigenstates and eigenvalues of Hamiltonian for a single electron and two electrons have been calculated using finite difference method and exact diagonalization technique. The effects of centrifugal potential and magnetic filed on electron localization and energy spectrum have been investigated for a single electron. For two electrons, the electron-electron interaction increases the energy levels significantly relative to the non-interacting electrons. It is found that the ground state includes both spin-singlet and spin-triplet states for interacting electrons, while for non-interacting case, the ground state includes only spin-singlet state. The period of Aharonov-Bohm oscillation for interacting electrons is equal to the half of that for non-interacting electrons which shows the fractional Aharonov-Bohm oscillations for interacting electrons. By calculating the addition energy, it is shown that the spin-singlet state is more stable

than that the spin-triplet states. The magnetization shows oscillatory behavior by increasing magnetic field and the electron-electron interaction decreases magnetization effect.

REFERENCES:

1. Tarucha S, Austing D G and Honda T, Van der Hage R J and L. P. Kouwenhoven, 1996 *Phys. Rev. Lett.* 77, 3613-6.
2. Reimann S M and Manninen M 2002 *Rev. Mod. Phys.* 74, 1283-1342
3. Aharonov Y, Bohm D 1959 *Phys. Rev.* 115, 485-90.
4. Webb R A, Washburn S, Umbach C P, Laibowitz R B 1985 *Phys. Rev. Lett.* 54, 2696-2699.
5. Timp G, Chang A M, Cunningham J E, Chang T Y, Mankiewich P, Behringer R, Howard R E 1987 *Phys. Rev. Lett.* 58, 2814-8.
6. Pedersen S, Hansen A E, Kristensen A, Shdersen C B, Lindelof P E 2000 *Phys. Rev. B* 61 5457-60.
7. Mano T, Kuroda T, Sanguinetti S, Ochiai T, Tateno T, Kim J, Noda T, Kawabe M, Sakoda K, Kido G and Koguchi N 2005 *Nano Lett.* 5, 425-8.
8. Chwiej T and Szafran B 2008 *Phys. Rev. B* 78 245306.
9. Castelano L K, Hai G Q, Partoens B and Peeters F M 2009 *J Appl Phys* 106 073702.
10. Kuroda T, Mano T, Ochiai T, Sanguinetti S, Sakoda K, Kido G and Koguchi N 2005 *Phys. Rev. B* 72 205301.
11. Fuhrer A, Lüscher S, Ihn T, Heinzel T, Ensslin K, Wegschneider W and Bichler M 2001 *Nature* 413, 822-5.
12. Keyser U F, Fuhner C, Borck S, Haug R J, Bichler M, Abstreiter G, Wegscheider W 2003 *Phys. Rev. Lett.* 90 196601.
13. Fuster G, Pacheco M and Barticevic Z 2004 Brazilian Journal of Physics 34 no. 2B 666-69.
14. Szafran B and Peeters F M 2005 *Phys Rev. B* 72 155316.
15. Planelles J and Climente J I 2005 *Eur. Phys. J. B* 48 65-70.
16. Climente J I and Planelles J 2005 *Phys. Rev. B* 72 155322.
17. Climente J I, Planelles J, Barranco M, Malet F and Pi M 2006 *Phys Rev. B* 73, 235327.
18. Malet F, Barranco M, Lipparini E, Mayol R and Pi M 2006 *Phys. Rev. B* 73, 245324.
19. Planelles J, Rajadell F, Climente J I, Royo M and Movilla J L 2007 *Journal of Physics, Conference Series* 61 936-41.
20. Culchac F J, Porras-Montenegro N, Granada J C and Latge A 2008 *Microelectronics Journal* 39 402-06.
21. Escartin J M, Malet F, Barranco M and Pi M 2010 *Physica E* 42 841-3.
22. Somaschini C, Bietti S, Sanguinetti S and Koguchi N 2009 *Nano Lett.* 9 10 3419-24.
23. Salehani K H, Esmaeilzadeh M and Shakouri K, 2010, JNanoR. 10, 121-130.
24. Kleemans N A J M, Bominaar-Silkens I M A, Fomin V M, Gladilin V N, Granados D, Taboada A G, Garcia J M, Offermans P, Zeitler U, Christianen P C M, Maan J C, Devreese J T and Koenraad P M 2007 *Phys. Rev. Lett.* 99 146808.
25. Byers N and Yang N C 1961 *Phys. Rev. Lett.* 7, 46.